Geophysical Research Letters

16 APRIL 2012 • Volume 39 Number 7

Articles published online 1 April – 15 April 2012

AGU American Geophysical Union

Special Section: The 11 March 2011 Tohoku-Oki Earthquake and Tsunami • Uranus's auroras observed from Hubble Space Telescope • Hurricane feedback research may improve intensity forecasts

The 2011 Japan tsunami current velocity measurements from survivor videos at Kesennuma Bay using LiDAR

Hermann M. Fritz,[1] David A. Phillips,[2] Akio Okayasu,[3] Takenori Shimozono,[3] Haijiang Liu,[4] Fahad Mohammed,[1] Vassilis Skanavis,[5] Costas E. Synolakis,[5,6] and Tomoyuki Takahashi[7]

Received 17 December 2011; accepted 20 December 2011; published 21 January 2012.

[1] On March 11, 2011, a magnitude M_w 9.0 earthquake occurred off the coast of Japan's Tohoku region causing catastrophic damage and loss of life. The tsunami flow velocity analysis focused on two survivor videos recorded from building rooftops at Kesennuma Bay along Japan's Sanriku coast. A terrestrial laser scanner was deployed at the locations of the tsunami eyewitness video recordings. The tsunami current velocities through the Kesennuma Bay are determined in a four step process. The LiDAR point clouds are used to calibrate the camera fields of view in real world coordinates. The motion of the camera during recordings was determined. The video images were rectified with direct linear transformation. Finally a cross-correlation based particle image velocimetry analysis was applied to the rectified video images to determine instantaneous tsunami flow velocity fields. The measured maximum tsunami height of 9 m in the Kesennuma Bay narrows were followed by maximum tsunami outflow currents of 11 m/s less than 10 minutes later. **Citation:** Fritz, H. M., D. A. Phillips, A. Okayasu, T. Shimozono, H. Liu, F. Mohammed, V. Skanavis, C. E. Synolakis, and T. Takahashi (2012), The 2011 Japan tsunami current velocity measurements from survivor videos at Kesennuma Bay using LiDAR, *Geophys. Res. Lett.*, *39*, L00G23, doi:10.1029/2011GL050686.

1. Introduction

[2] On March 11, 2011, at 05:46:23 UTC (local time 02:46:23 pm), a magnitude M_w = 9.0 earthquake occurred off the coast of Japan's Tohoku region about 130 km east of Sendai [*Simons et al.*, 2011; *Fujii et al.*, 2011]. This represents the fourth largest earthquake instrumentally recorded. The earthquake and tsunami caused substantial damage and loss of life along Japan's coastline followed by multiple melt-downs at the Fukushima nuclear power plant [*Bowyer et al.*, 2011]. The bulk of the 19,447 fatalities (15,840 dead and 3,607 missing presumed dead) were concentrated in the coastal regions of Myagi, Iwate and Fukushima prefectures (http://www.npa.go.jp/archive/keibi/biki/higaijokyo_e.pdf; http://www.47news.jp/CN/201104/CN2011041901000540.html). The majority at 92.5% of the fatalities are attributed to the tsunami. The 2011 Tohoku tsunami represents Japan's deadliest tsunami since the 1896 Meiji-Sanriku tsunami earthquake [*Tanioka and Satake*, 1996]. For the 2011 Tohoku tsunami we measured a maximum tsunami runup exceeding 38 m along the Sanriku coast in a narrow valley at Aneyoshi, Iwate Prefecture (http://www.coastal.jp/tsunami2011/) [*Mori et al.*, 2011]. Extreme runup heights were observed along the Sanriku coast in the past with 38 m by the 1896 Meiji tsunami and 29 m by the 1933 Showa tsunami [*Matsuo*, 1933]. These historic Sanriku tsunamis had limited impact further south, while the 869 Jogan earthquake produced large tsunami inundation distances up to a few kilometers preserved in sediment deposits in the Sendai plain [*Minoura et al.*, 2001; *Sawai et al.*, 2008; *Satake et al.*, 2008]. Forecasts by the Earthquake Research Committee (ERC) for the Tohoku region were based on historical earthquakes and limited to estimated earthquake magnitudes up to M∼8.2 [*Fujii et al.*, 2011]. Tsunami mitigation and evacuation plans, coastal structures and vertical evacuation sites were designed based on these too conservative forecasts.

2. Post-Tsunami Reconnaissance

[3] Several tsunami reconnaissance trips were conducted in Japan (http://www.coastal.jp/tsunami2011/). This report focuses on the surveys at tsunami eyewitness video recording locations in Kesennuma and the subsequent video image calibration, processing and tsunami flow velocity analysis. Kesennuma is a city located in the northeast of Miyagi Prefecture and borders Iwate Prefecture with Hiroata Bay and Rikuzentakata City 12 km to the north-northeast (Figure 1). Kesennuma is situated on the western side of Kesennuma Bay, which includes Oshima Island. Kesennuma Bay represents one of the many rias characterizing the Sanriku coast. The collision of the Kuroshio and Oyashio ocean currents along the Sanriku coast make it one of the most productive fisheries in the world with Kesennuma being one of the main fishing harbors. Kesennuma Bay has been impacted by the 1896 Meiji-Sanriku, 1933 Showa-Sanriku, 1960 and 2010 Chile tsunamis making it one of Japan's most vulnerable cities for both near- and far-field tsunamis [*Tsuji et al.*, 2010; *Fritz et al.*, 2011; T. Saijou, Field survey report of the Chilean tsunami, Miyagi Prefecture (in Japanese), 1961, available at http://tsunami.media.gunma-u.ac.jp/xml_tsunami/xmlindex.php?info=65%20reportMetatab%20reportSectab]. Residents

[1]School of Civil and Environmental Engineering, Georgia Institute of Technology, Savannah, Georgia, USA.
[2]UNAVCO, Boulder, Colorado, USA.
[3]Department of Ocean Sciences, Tokyo University of Marine Science and Technology, Tokyo, Japan.
[4]Department of Civil Engineering, University of Tokyo, Tokyo, Japan.
[5]Department of Environmental Engineering, Technical University of Crete, Chanea, Greece.
[6]Department of Civil and Environmental Engineering, University of Southern California, Los Angeles, California, USA.
[7]Department of Safety Science, Kansai University, Osaka, Japan.

0094-8276/12/2011GL050686

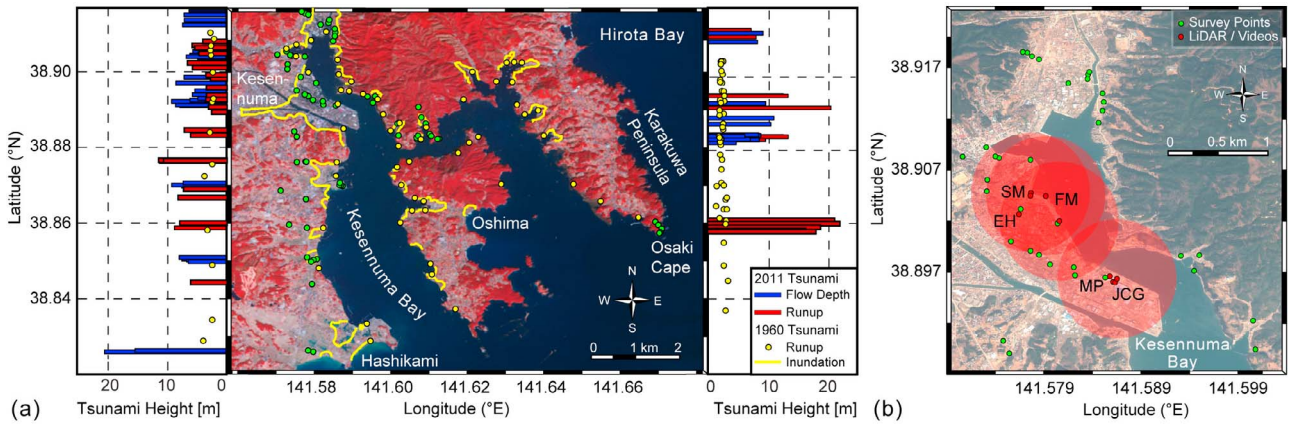

Figure 1. Kesennuma Bay: (a) measured tsunami flow depths and runup heights for the 2011 Tohoku and 1960 Chile events (ASTER satellite image acquired March 14, 2011); (b) TLS instrument and eyewitness camera man positions at Japanese Coast Guard (JCG) and Miyagi Prefecture (MP) buildings, fish market vertical evacuation platform (FM), shark museum (SM), and an evacuation hill (EH). Transparent red circles indicate approximate coverage areas in LiDAR scans (WORLDVIEW-2 satellite image acquired March 20, 2011).

along the Sanriku coast are acutely aware of tsunamis. Every year in June an evacuation exercise is held in Kesennuma commemorating the 1896 event. The emergency manager Ken-Ichi Sato pressed the tsunami alarm button at Kesennuma within 2 minutes of the earthquake prior to the first official warnings issued by the Japan Meteorological Agency (JMA) and the Pacific Tsunami Warning Center (PTWC). Despite this extraordinary level of tsunami preparedness at Kesennuma, 1467 residents were killed in the 2011 tsunami (973 confirmed dead and 494 missing presumed dead). The fatality rate was 2.3% out of a population of 63,841 (http://www.npa.go.jp/archive/keibi/biki/higaijokyo_e.pdf). Some 20,000 houses were destroyed or damaged. In addition, 500 fishing boats were lost at Kesennuma.

[4] The Kesennuma surveys we report took place using two survey groups from April 14 to 16 and June 12 to 14, 2011. The first survey team documented tsunami runup, flow depth and inundation; wave induced deposition or erosion, structural damage and interviewed eyewitnesses using established protocols [*Synolakis and Okal,* 2005]. Watermarks were surveyed with a Trimble GPS rover connected via Bluetooth to a laser range finder (Lasercraft XLRic) to record offset points and differentially corrected during post-processing with the base station network of the Geospatial Information Authority of Japan (GSI). The Kesennuma survey recorded 77 tsunami runup and flow depth measurements (Table S1 of the auxiliary online material).[1] At most locations, the tsunami arrived as sea levels passed through low-tide. Measured data are presented relative to Tokyo Peil (T.P. datum corresponds to mean sea level of Tokyo Bay). A significant variation in tsunami impact was observed from the entrance to the head of the Kesennuma Bay (Figure 1a). The tsunami impact peaked with a localized maximum tsunami height of 20 m measured on a tree at Hashikami on the headland to the west of the Kesennuma Bay entrance and runup heights of approximately 20 m on Osaki Cape separating Kesennuma from Hirota Bay. The tsunami heights remained below 10 m within the city of Kesennuma. On the mainland across the narrow channel facing the backside of Oshima Island a localized maximum runup of 20 m was measured in a narrow valley. This is reminiscent of the Babi Island effect observed near Flores, Indonesia [*Yeh et al.,* 1994]. The 2011 Tohoku tsunami heights approximately quadrupled the 1960 Chile tsunami heights at Kesennuma (http://tsunami.media.gunma-u.ac.jp/xml_tsunami/xmlindex.php?info=65%20reportMetatab%20reportSectab). Eyewitnesses at Hashikami at the entrance to Kesennuma Bay reported the first tsunami wave arrival within 30 minutes of the earthquake and up to 3 waves.

3. Terrestrial Laser Scanning

[5] A follow-up survey of Kesennuma from June 12 to 14, 2011 focused on terrestrial laser scanning, TLS, at locations with high quality eyewitness videos. We acquired precise topographic data using TLS at three sites in Kesennuma: the Japanese Coast Guard building, the fish market vertical evacuation platform and a downtown street as seen from an evacuation hill (Figure 1b). Multiple scans were acquired from a total of 9 TLS instrument positions. Here we only discuss the Japanese Coast Guard (JCG) and Miyagi Prefecture (MP) building sites at the narrowest section of Kesennuma Bay (Figure 2). The TLS technology is based on Light Detection and Ranging (LiDAR) and is also referred to as ground-based LiDAR or tripod LiDAR [*Jacobs*, 2005]. The LiDAR measurements, combined with the orientation and position of the scanner, produce a 3-dimensional "point cloud" dataset. The addition of digital photography yields photorealistic 3D images. Integrated GPS measurements allow accurate georeferencing of TLS data in an absolute reference frame such as WGS84 [*Wang et al.*, 2011].

[6] We deployed a Riegl VZ-400, which is a time-of-flight based scanner that utilizes a near infrared (1550 nm) laser with a beam divergence of 0.3 mrad (30 mm increase of beamwidth per 100 m of range). This scanner has an

[1]Auxiliary materials are available in the HTML. doi:10.1029/2011GL050686.

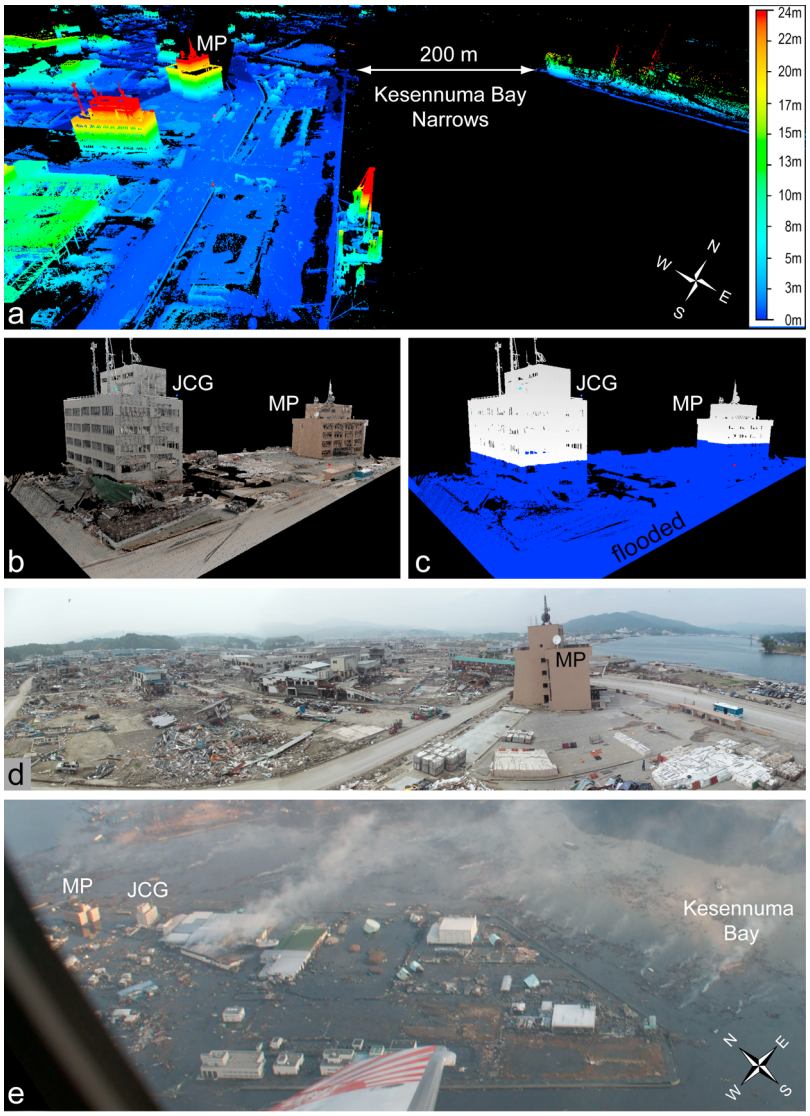

Figure 2. Kesennuma Bay narrows with Japanese Coast Guard (JCG) and Miyagi Prefecture (MP) buildings: (a) Terrestrial Laser Scanning (TLS) point cloud across Kesennuma Bay with colored elevation; (b) LiDAR point cloud with photographic true colors; (c) JCG and MP vertical evacuation buildings with maximum water level; (d) tsunami aftermath with massive infrastructure damage and destruction; (e) aerial view of on March 12, 2011 (photo credit: Kenji Satake, ERI, University of Tokyo).

effective measurement rate of 42,000 meas/sec (long range mode). Its effective measurement range varies from 600 m to 280 m for natural targets with reflectivities of $\geq$ 90% to $\geq$ 20%, respectively. The specified measurement accuracy is 5 mm and its stated precision is 3 mm. Photographic imagery was acquired using a Nikon D700 DSLR camera with 20 mm lens was mounted to the top of the scanner via a calibrated mount. The scanner and DSLR camera were controlled with the Riegl Riscan Pro software.

[7] Our general TLS data acquisition strategy was to scan from multiple locations ("scan positions") chosen to match the eyewitness video vantage point(s) and to generate LiDAR point clouds with desired point densities and minimal shadows. At the Kesennuma Bay narrows, we collected TLS data from four scan positions with two of the scan positions located on the roof of the JCG building. From each scan position, we would acquire one or more laser scans in order to achieve the desired spatial coverage and point density. Seven calibrated LiDAR targets ("tie points") were deployed at locations visible from various scan positions in order to register the different scans into a common coordinate system. Four of these targets were affixed with GPS antennas recording ~4 hour static GPS sessions.

[8] TLS data were processed using the Riscan Pro software. An important part of the post processing included the incorporation of the GPS measurements in order to improve the scan position registrations performed in the field and to georeference the merged point cloud. Precise GPS baseline measurements were computed using Trimble Geomatics Office (TGO) software. The GPS Online Positioning User Service (OPUS) provided by the U.S. National Geodetic Survey (NGS) was used to acquire coordinates of the tie point (named KCG1) that was used as the control point in TGO. At the Kesennuma Bay narrows, all four scan

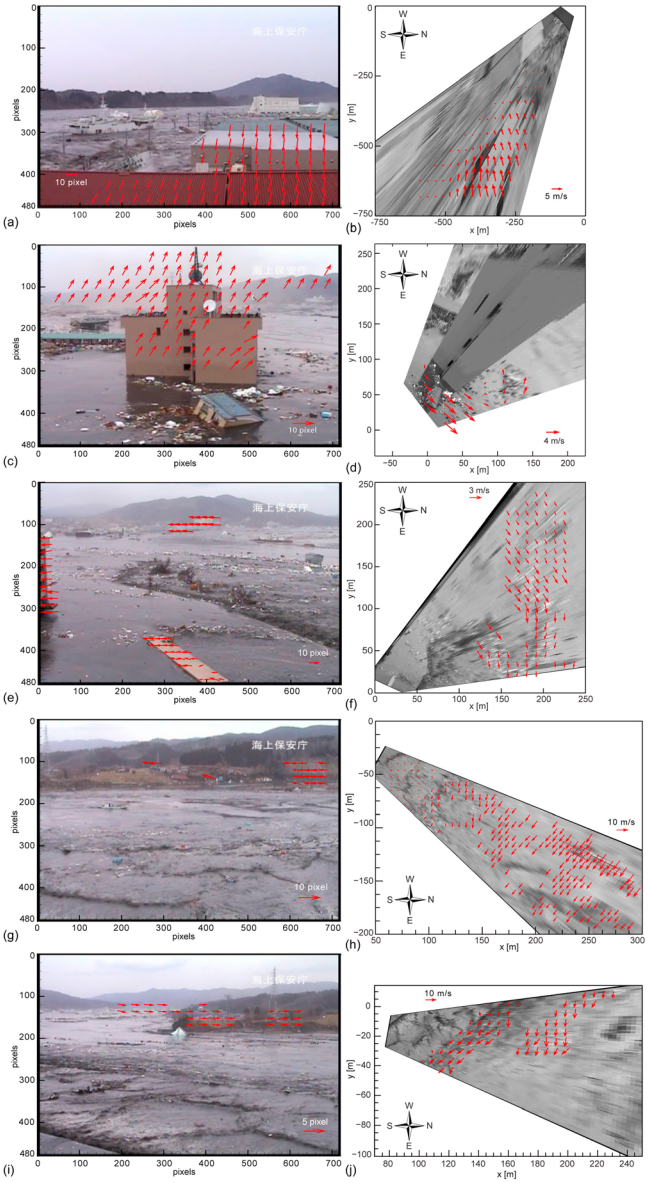

Figure 3. Tsunami JCG-video analysis: Figures 3a, 3c, 3e, 3g, and 3i show raw video image with selected ground control points and computed camera motion; Figures 3b, 3d, 3f, 3h, and 3j show rectified video image with computed instantaneous tsunami flow velocity vector field; recording time (a, b) during flooding at 15:29:53, and during outflow at (c, d) 15:36:22, (e, f)15:40:15, (g, h)15:42:33, and (i, j) 15:42:43 JST.

positions were merged into a common reference frame with a reported standard deviation of 0.002 m (estimated registration error) in Riscan Pro. WGS84 is used as the global coordinate system with elevations converted to mean sea level. The combined point clouds from all four scans with colored elevation across the Kesennuma Bay narrows are shown in Figure 2a. Detailed three dimensional images of the JCG and MP buildings with photorealistic colors and maximum tsunami flood level are shown in Figures 2b and 2c. The rooftops of the JCG and MP buildings served successfully as vertical evacuation platforms. The LiDAR derived measurements presented here are based exclusively on analysis of the actual point cloud data, which consists of 119 million LiDAR points at the JCG site alone.

4. Tsunami Video Processing

[9] Copies of the original full length video recordings at Kesennuma were received during a visit at the Japanese Coast Guard headquarters in Miyagi Prefecture. Two video sequences with durations of 54 min. 57 s and 5 min. 44 s were analyzed, synchronized and referenced in time (JST = UTC+9). The two overlapping video recording positions were located on the rooftop of the JCG and MP buildings (Figure 2). The massive reinforced concrete structures of the JCG and MP buildings served successfully as vertical evacuation platforms saving many lives while the surrounding area is characterized by massive destruction (Figure 2d).

[10] The analysis of the tsunami videos follows a four step procedure developed for the analysis of 2004 Indian Ocean tsunami videos at Banda Aceh, Indonesia [*Fritz et al.*, 2006]. The first step requires the calibration of the sector of view present in the eyewitness video recordings, which is of critical importance in order to extract quantitative tsunami flow velocity information. The camera calibration task was complicated by the fact that the recordings were shot with handheld amateur video cameras by survivors under extreme stress. The photogrammetric transformation between the 3-D world and 2-D image coordinates requires the input of both the world coordinates (3-D space) and the image coordinates (2-D plane) of visually identifiable ground control points. The real world coordinates and elevations of objects suitable for ground control points in tsunami inundation videos were measured in the LiDAR point cloud data.

[11] In a second step the video image motion induced by the panning of the video camera was determined from subsequent raw color images by means of planar particle image velocimetry (PIV). Prior to the PIV-analysis the steady image areas with fixed objects above the flood level were isolated from the rest of the image with digital masks. The instantaneous planar displacement fields attributed to camera motion are computed with a cross-correlation based adaptive multi-pass algorithm with decreasing window sizes, window deformations, window offsets and subpixel interpolations of the correlation peaks [*Raffel et al.*, 1998; *Fritz et al.*, 2003]. The determined camera motion is superimposed on raw images shown in Figures 3a, 3c, 3e, 3g, and 3i).

[12] The third step involves the transformation of the raw tsunami video images from image coordinates to world coordinates, which preceded the PIV tsunami flow velocity analysis to avoid any physical distortion. The mapping from video frame to real world coordinates follows the direct linear transformation (DLT) procedure [*Holland et al.*, 1997]. The DLT coefficients are linearized parameters of the collinear relationship between each image coordinates and its corresponding world coordinates. The DLT coefficients are determined from the ground control points by using a least squares method. Given the pre-determined DLT coefficients, the transformation of image coordinates to world coordinates was applied by constraining the elevation z in real coordinates to the measured tsunami surface. This assumption limits the transformation to a planar tsunami surface and neglects local surface elevation features.

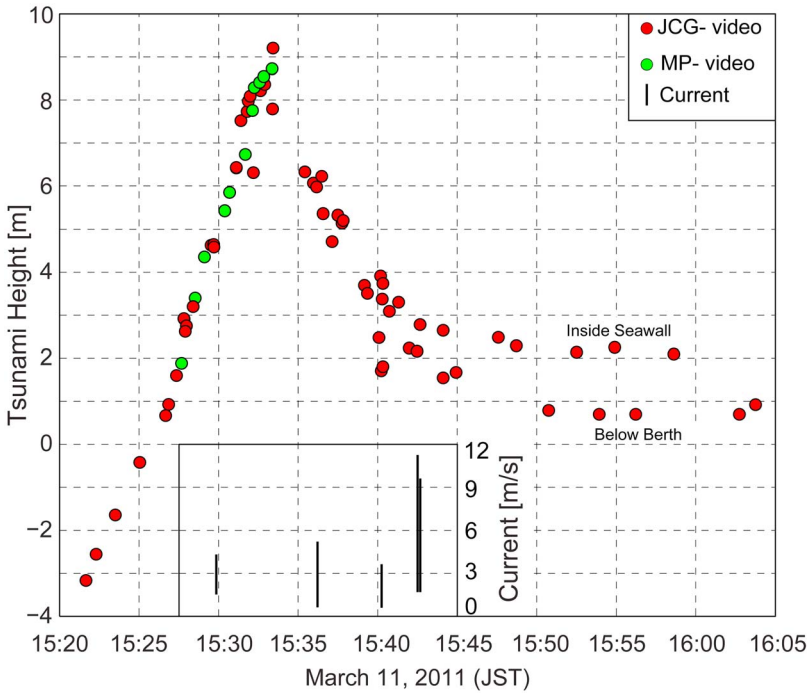

Figure 4. Tsunami height time series derived from the combined MP and JCG videos with ranges of tsunami currents in insert for times shown in Figure 3.

The tsunami video images were rectified accordingly and resampled to convert the rectified images onto a regular pixel matrix. Rectified tsunami video image maps form the background of the tsunami flow velocity vector fields (Figures 3b, 3d, 3f, 3h, and 3j). The significantly oblique viewing angles and the wide camera angles of view result in massive distortions of the raw video images during the rectification process.

[13] Finally, the tsunami surface current and flooding velocity vector maps are determined by applying the digital PIV analysis method to the rectified tsunami video images with floating debris clusters. In previous studies the PIV method was successfully applied to granular landslide surfaces with non-discrete image patterns [*Fritz et al.*, 2009] as well as near shore flow structures in the swash zone [*Holland et al.*, 2001]. Similarly, herein we applied the cross-correlation based PIV analysis to subsequent tsunami inundation images resulting in instantaneous tsunami velocity vector fields during flooding (Figure 3b) and outflow (Figures 3d, 3f, 3h, and 3j). A video derived tsunami height time series based on water surface elevations at surface piercing objects and ranges of measured tsunami currents are shown in Figure 4. The JCG video starts with the end of the initial drawdown at a water level of about −3 m followed by 12 minutes of flooding with an average water level increase of 1 m/minute. The maximum tsunami height in the Kesennuma Bay narrows reaches 9 m at 15:33 (JST). The water surface currents are close to zero at the time of maximum tsunami height due to reversal of primary flow direction from in- to outflow. The drawdown after the maximum tsunami height continues for 18 minutes followed by a sequence of secondary in- and outflows. Maximum tsunami outflow currents of 11 m/s were measured less than 10 minutes after the maximum tsunami height inside the navigation channel at Kesennuma Bay narrows. The instantaneous maximum tsunami outflow current increases from just over 3 m/s to 11 m/s within little more than 2 minutes making safe navigation through the Kesennuma Bay narrows impossible for any type of vessel. The Froude number $F = v/\sqrt{gh}$ approaches $F \approx 1$ with a typical water depth of 10 m inside the navigation channel at the Kesennuma Bay narrows at the time of maximum outflow currents. The standing water surface waves inside the navigation channel at the Kesennuma Bay narrows confirm the transcritical flow regime with $F \approx 1$ [*Fritz and Hager*, 1998].

5. Summary and Conclusions

[14] The rapid response of the survey teams to Kesennuma after the March 11, 2011 event resulted in the recovery of important data on the characteristics of the tsunami effects and inundation of a major port city in the tsunami near field. The analysis focused on two survivor videos recorded from building rooftops at the Kesennuma Bay narrows. The LiDAR scanning from multiple positions at the locations of the tsunami eyewitness video recordings allowed to calibrate the camera fields of view in real world coordinates. The tsunami current velocities through the Kesennuma Bay narrows were determined in a four step process involving: calibration of the camera fields of view, determination of the camera motion with PIV, rectification of the video images with direct linear transformation (DLT), determination of the tsunami current with surface PIV on the rectified images. The measured tsunami outflow velocities up to 11 m/s make navigation impossible.

[15] **Acknowledgments.** The survey team was supported by the National Science Foundation through the NSF RAPID award CMMI-1135768. The Riegl VZ-400 terrestrial laser scanner, four Topcon GB-1000 dual frequency GPS receivers, and Topcon PGA1 antennas were from the UNAVCO instrument pool.

References

Bowyer, T. W., S. R. Biegalski, M. Cooper, P. W. Eslinger, D. Haas, J. C. Hayes, H. S. Miley, D. J. Strom, and V. Woods (2011), Elevated radioxenon detected remotely following the Fukushima nuclear accident, *J. Environ. Radioact.*, *102*, 681–687, doi:10.1016/j.jenvrad.2011.04.009.

Fritz, H. M., and W. H. Hager (1998), Hydraulics of embankment weirs, *J. Hydraul. Eng.*, *124*(9), 963–971, doi:10.1061/(ASCE)0733-9429(1998)124:9(963).

Fritz, H. M., W. H. Hager, and H.-E. Minor (2003), Landslide generated impulse waves: Part 1: Instantaneous flow fields, *Exp. Fluids*, *35*, 505–519, doi:10.1007/s00348-003-0659-0.

Fritz, H. M., J. C. Borrero, C. E. Synolakis, and J. Yoo (2006), 2004 Indian Ocean tsunami flow velocity measurements from survivor videos, *Geophys. Res. Lett.*, *33*, L24605, doi:10.1029/2006GL026784.

Fritz, H. M., F. Mohammed, and J. Yoo (2009), Lituya Bay landslide impact generated mega-tsunami 50th anniversary, *Pure Appl. Geophys.*, *166*(1–2), 153–175, doi:10.1007/s00024-008-0435-4.

Fritz, H. M., et al. (2011), Field survey of the 27 February 2010 Chile tsunami, *Pure Appl. Geophys.*, *168*(11), 1989–2010, doi:10.1007/s00024-011-0283-5.

Fujii, Y., K. Satake, S. Sakai, M. Shinohara, and T. Kanazawa (2011), Tsunami source of the 2011 off the Pacific coast of Tohoku, Japan earthquake, *Earth Planets Space*, *63*(7), 815–820, doi:10.5047/eps.2011.06.010.

Holland, K. T., R. A. Holman, and T. C. Lippmann (1997), Practical use of video imagery in neareshore oceanographic field studies, *IEEE J. Oceanic Eng.*, *22*(1), 81–92, doi:10.1109/48.557542.

Holland, K. T., J. A. Puleo, and T. N. Kooney (2001), Quantification of swash flows using video-based particle image velocimetry, *Coastal Eng.*, *44*, 65–77, doi:10.1016/S0378-3839(01)00022-9.

Jacobs, G. (2005), Laser scanning: Big advantages, even for small projects, *Prof. Surv.*, *25*(10), 30–35.

Matsuo, H. (1933), Sanriku tsunami survey report, *Rep. Publ. Works Res. Stn., 24*, 83–136 (in Japanese).

Minoura, K., F. Imamura, D. Sugawara, Y. Kono, and T. Iwashita (2001), The 869 Jogan tsunami deposit and recurrence interval of large-scale tsunami on the Pacific coast of northeast Japan, *J. Nat. Disaster Sci.*, *23*(2), 83–88.

Mori, N., T. Takahashi, T. Yasuda, and H. Yanagisawa (2011), Survey of 2011 Tohoku earthquake tsunami inundation and run-up, *Geophys. Res. Lett.*, *38*, L00G14, doi:10.1029/2011GL049210.

Raffel, M., C. E. Willert, and J. Kompenhans (1998), *Particle Image Velocimetry – A Practical Guide*, Springer, Berlin.

Satake, K., Y. Namegaya, and S. Yamaki (2008), Numerical simulation of the AD 869 Jogan tsunami in Ishinomaki and Sendai plains (in Japanese with English abstract), *Ann. Rep. Active Fault Paleoearthquake Res.*, *8*, 71–89.

Sawai, Y., M. Shishikura, and J. Komatsubara (2008), A study on paleotsunami using hand corer in Sendai plain (Sendai City, Natori City, Iwanuma City, Watari Town, Yamamoto Town), Miyagi Prefecture, Japan, in *Annual Report on Active Fault and Paleoearthquake Research*, *Geol. Surv. Jpn.*, *8*, 17–70.

Simons, M., et al. (2011), The 2011 magnitude 9.0 Tohoku-oki earthquake: Mosaicking the megathrust from seconds to centuries, *Science*, *332*, 1421–1425, doi:10.1126/science.1206731.

Synolakis, C. E., and E. A. Okal (2005), 1992–2002: Perspective on a decade of post-tsunami surveys, in *Tsunamis: Case Studies and Recent Developments*, edited by K. Satake, *Adv. Nat. Technol. Hazards*, vol. 23, pp. 1–30, Springer, New York.

Tanioka, Y., and K. Satake (1996), Fault parameters of the 1896 Sanriku tsunami earthquake estimated from tsunami numerical modeling, *Geophys. Res. Lett.*, *23*(13), 1549–1552, doi:10.1029/96GL01479.

Tsuji, Y., T. Takahashi, and K. Imai (2010), Comparison of tsunami height distributions of the 1960 and the 2010 Chilean earthquakes on the coasts of the Japanese Islands, Abstract G36A-0832 presented at 2010 Fall Meeting, AGU, San Francisco, Calif., 13–17 Dec.

Wang, G., D. Phillips, J. Joyce, and F. O. Rivera (2011), The integration of TLS and continuous GPS to study landslide deformation: A case study in Puerto Rico, *J. Geod. Sci.*, *1*(1), 25–34, doi:10.2478/v10156-010-0004-5.

Yeh, H., P. L.-F. Liu, M. Briggs, and C. E. Synolakis (1994), Propagation and amplification of tsunamis at coastal boundaries, *Nature*, *372*(6504), 353–355, doi:10.1038/372353a0.

H. M. Fritz and F. Mohammed, School of Civil and Environmental Engineering, Georgia Institute of Technology, Savannah, GA 31407, USA. (fritz@gatech.edu; fahd@gatech.edu)

H. Liu, Department of Civil Engineering, University of Tokyo, 7-3-1 Hongo, Bunkyo-ku, Tokyo 113-8656, Japan. (hjliu@coastal.t.u-tokyo.ac.jp)

A. Okayasu and T. Shimozono, Department of Ocean Sciences, Tokyo University of Marine Science and Technology, 4-5-7 Konan, Minato-ku, Tokyo 109-0075, Japan. (okayasu@kaiyodai.ac.jp; shimo@kaiyodai.ac.jp)

D. A. Phillips, UNAVCO, 6350 Nautilus Dr., Boulder, CO 80301, USA. (phillips@unavco.org)

V. Skanavis, Department of Environmental Engineering, Technical University of Crete, Chanea 73100, Greece. (billskan@gmail.com)

C. E. Synolakis, Department of Civil and Environmental Engineering, University of Southern California, Los Angeles, CA 90089, USA. (costas@usc.edu)

T. Takahashi, Department of Safety Science, Kansai University, Osaka 569-1098, Japan. (tomot@kansai-u.ac.jp)